Dynamics and Evolution of Structure in Fiber Extrusion

JIRO SHIMIZU,[1] TAKESHI KIKUTANI[2]

[1] Yamagata College of Industry and Technology, Yamagata, Japan

[2] Department of Organic and Polymeric Materials, Graduate School of Science and Engineering, Tokyo Institute of Technology, Tokyo, Japan

Received 8 November 2000; accepted 18 November 2000

ABSTRACT: This paper gives a review of scientific advances in the understanding of the mechanism of fiber structure development in the high-speed melt spinning process. Research in this field has been active since the late 1970s. Particular attention is paid to the molecular orientation and orientation-induced crystallization occurring in the high-speed spinning process of poly(ethylene terephthalate), polyamides, and some other types of polymers. Characteristics of crystalline morphology developed in the spin line and evolution of structural variation in the cross-section of the fiber are also discussed. On-line measurement of the spin line revealed that fiber structure development is accompanied with neck-like deformation. Detailed behavior of the neck-like deformation such as diameter profile, necking temperature, and necking draw ratio are presented, and the relation between the neck-like deformation and the structure development is also discussed. © 2002 John Wiley & Sons, Inc. J Appl Polym Sci 83: 539–558, 2002

Key words: high-speed melt spinning; orientation-induced crystallization; neck-like deformation; structure development; poly(ethylene terephthalate)

INTRODUCTION

Several decades have passed since Carothers published an article on the synthesis of nylon-66 and synthetic fibers produced by melt spinning.[1] For thermoplastic polymers, such as polyesters, polypropylene (PP), and polyamides (NY 6, 66, etc.), melt spinning is the most useful method. Melt spinning also provides a technique for producing various kinds of polymer structures.[2]

Fiber processing is made up of three basic operations characterized by different principles. 1. Basic operation: spinning, drawing, and annealing. 2. Basic principle: shape-formation, orientation, and crystallization.

From the 1960s, du Pont and Ziabicki showed that the drawing and annealing operations can be omitted if spinning is done at high speed.[3,4] In the 1960s, the direct spin-draw process was developed commercially. In the 1970s, partially oriented yarn (POY) spun by a spinning speed of 3000–3500 m/min was started to be used as the feed yarn for the draw-texturing process.[5,6]

In 1977, Shimizu et al.[7] reported that polyethylene terephthalate (PET) yarn having a highly oriented and crystallized structure was obtained by high-speed spinning of 5000–7000 m/min, and the mechanism of structure formation was explained based on the orientation-induced crystallization in the spin line. 1. Basic operation: high speed spinning; 2. basic principle: orientation-induced crystallization. Today, high-speed spinning of 6000–7000 m/min is in commercial operation for the production of PET and nylon yarns.[5]

EVOLUTION OF FIBER STRUCTURE

Physical properties and structure of PET yarns spun at various speeds are summarized below.[8,9]

Correspondence to: J. Shimizu.

Journal of Applied Polymer Science, Vol. 83, 539–558 (2002)

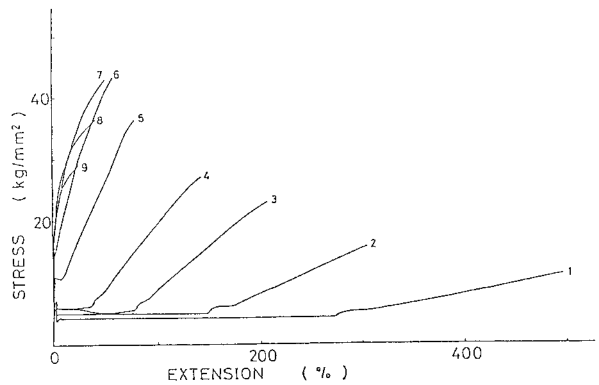

Figure 1 Stress–strain curves of PET fibers prepared at various spinning speeds.[10]

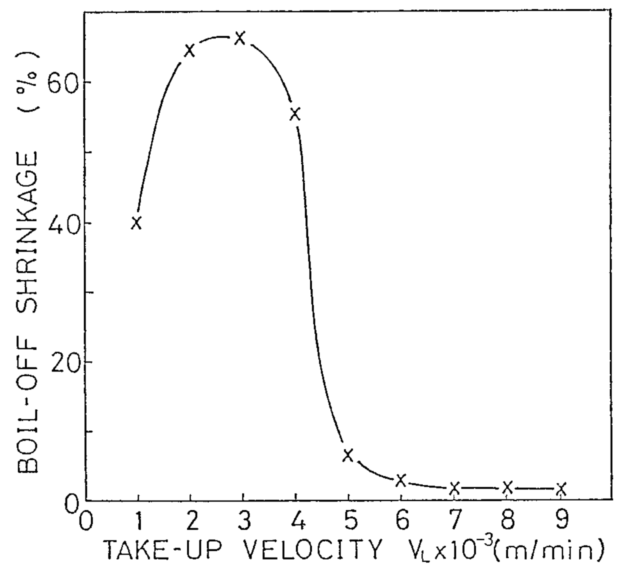

Figure 3 Dependence of boil-off shrinkage of PET yarn on spinning speed.[10]

General Properties of Yarns

Mechanical Property

Figure 1 shows the stress–strain (s–s) curve of PET yarn spun at various speeds.[10] The tenacity generally increases and the elongation generally decreases as the spinning speed increases. The PET yarn can be classified into two groups from the shape of the s–s curve, that is, the as-spun yarn obtained below 4000 m/min has the yield point (UDY, POY) and the region of constant load elongation (UDY).[6–9]

Characteristics of high-speed spun yarn obtained above 5000 m/min include unclear yield point, and the s–s curve becomes similar to that of conventional PET yarn (FOY). The tenacity reaches a maximum value at 6000–7000 m/min and then decreases up to 8000–9000 m/min, as shown in Figure 1.

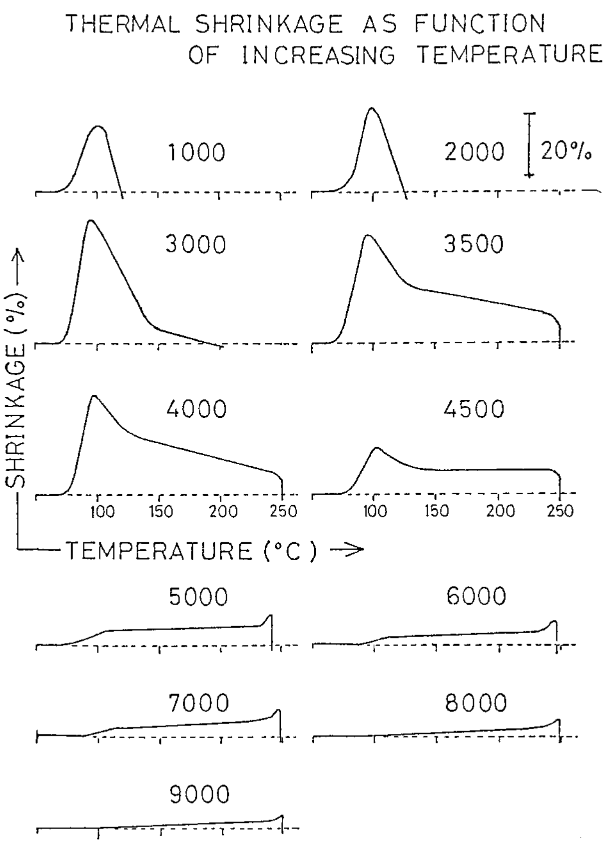

Figure 2 Thermal shrinkage for as-spun PET yarn produced at 1000–9000 m/min.[11]

Thermal Property

Thermal property is a very important characteristic for textile processing and strongly relates to the fiber structure. Figure 2 shows thermal shrinkage of spun yarn produced at various spinning speeds as a function of temperature.[2,11] (a) The shrinkage starts from the glass transition temperature; (b) the maximum shrinkage of each curve below 4000 m/min appears at ca. 100°C, and its maximal value exhibits at 3000 m/min; (c) the shrinkage for yarn produced at high speed over 5000 m/min is very small.

These results agree with the data obtained by boil-off shrinkage of Figure 3. The shrinkage exhibits maximum at spinning speed of 2000–3000 m/min, and then decreases to 2–3% at speeds over 6000 m/min. The high-speed spun PET yarn has good thermal stability.[10]

The above changes of physical property of as-spun PET yarn are attributed to the structure

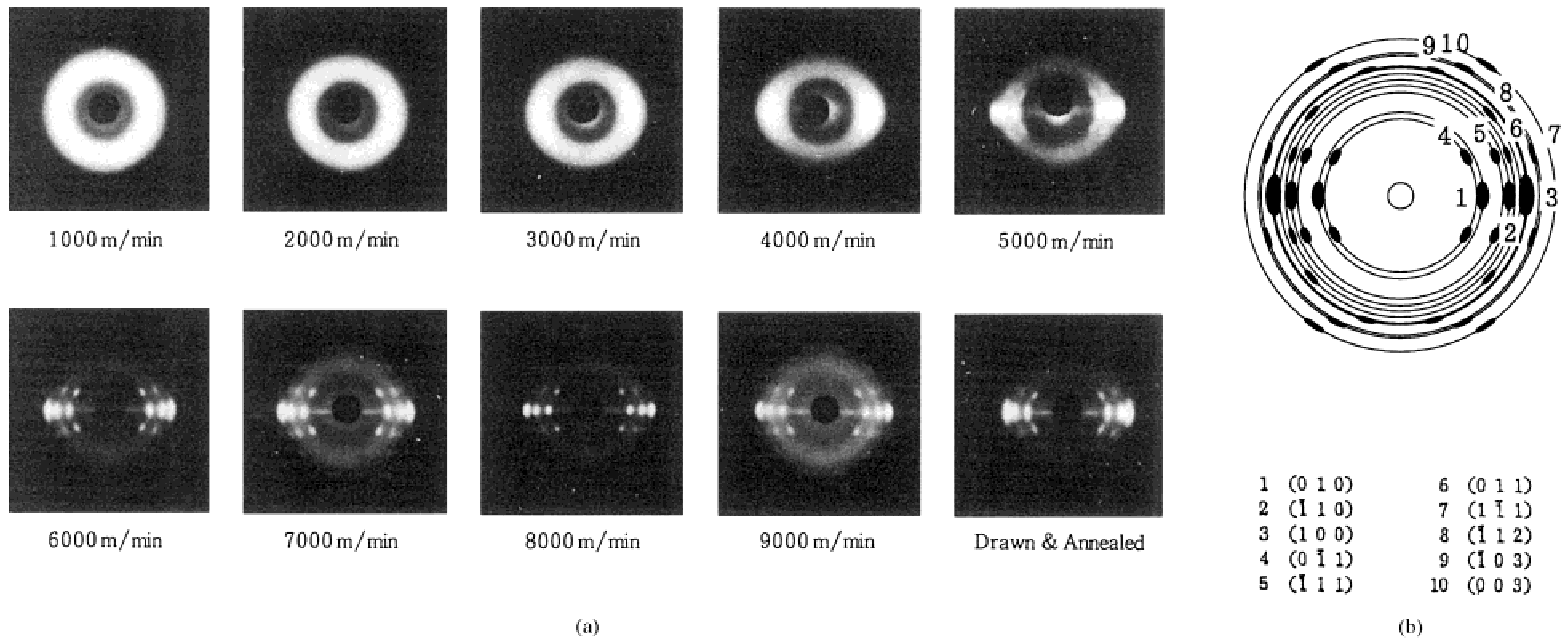

Figure 4 (a) The WAXS pattern of as-spun PET yarn produced at each spinning speed.[10,14] (b) The WAXS pattern calculated from the crystal unit cell parameters of PET.[13]

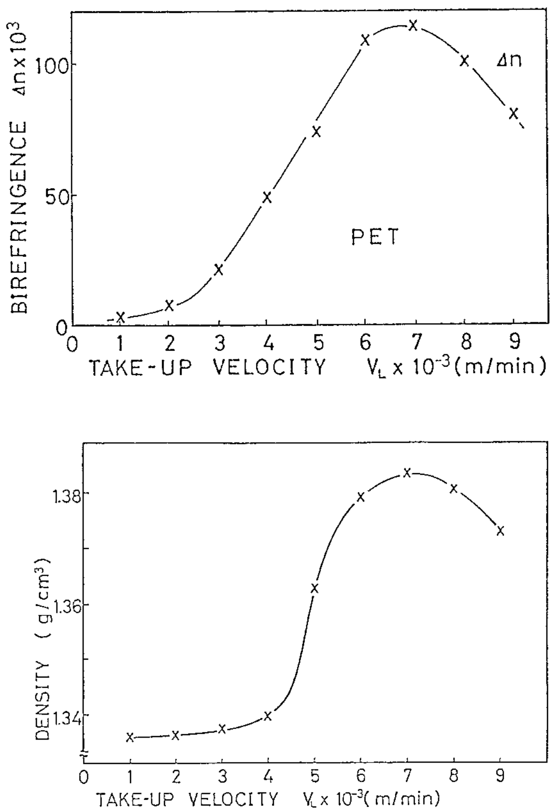

Figure 5 Birefringence (Δn) and density of PET as-spun yarn produced at various spinning speeds.[10,15]

given by the increase of spinning speed. Over 4000 m/min, we think, the orientation induced crystallization occurs in a spin line, and this structure gives stabilization to the yarn.[7]

Orientation and Crystal Structure

The molecular chain aligns along the fiber axis and crystallizes in spin line, and in this manner the fiber structure is developed.

Wide-Angle X-ray Diffraction Pattern

The crystal structure was analyzed from X-ray diffraction study.

The unit cell of PET is triclinic, and the molecular chain is almost fully extended along the *c* axis.[12]

Figure 4(b) shows the wide-angle X-ray scattering (WAXS) pattern calculated from the crystal unit cell of PET.[13]

Figure 4(a) shows the WAXS patterns of as-spun PET yarn produced at various spinning speeds. Drawn & annealed is a conventional drawn and annealed yarn (FOY). Both physical properties described above are related to a fine structure shown by WAXS patterns.

The WAXS pattern of the as-spun yarn below 4000 m/min shows diffuse reflection, and reveals that these yarns are amorphous.

The WAXS pattern of 5000–9000 m/min shows the reflection from the crystal, and a more distinct crystalline pattern with increase of spinning speed.

Molecular Orientation and Crystallization

With increase of spinning speed, the PET yarn changes from a low-oriented amorphous yarn to a highly oriented crystalline yarn.[7]

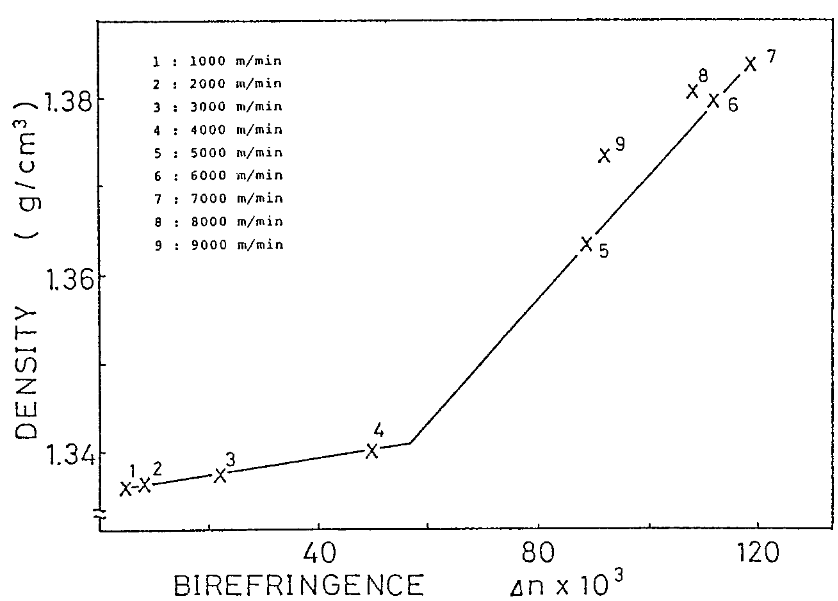

Figure 6 Relation between Δn and density of PET yarn.[10,15]

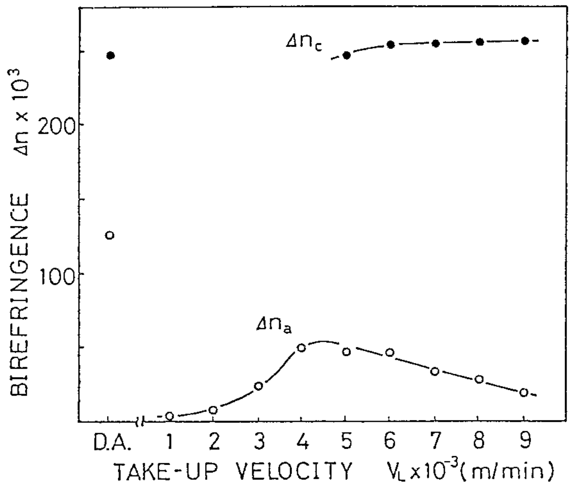

Figure 7 Crystal and amorphous orientation of PET yarn as a function of spinning speed.[15]

Figure 5 shows the dependence of birefringence (Δn) and density upon increase of spinning speed. These values respectively represent the molecular orientation and crystallinity. Δn shows a sigmoidal increase with spinning speed, and reaches a maximum value $\Delta n = 0.12$ at 7000 m/min.

On the other hand, density shows an abrupt increase between 4000 and 5000 m/min, and reaches a maximum value also at 7000 m/min.

Figure 6 shows the relation between density and Δn, and we find a break point at $\Delta n = 0.055$. These results suggest that orientation-induced crystallization starts at about 5000 m/min.[7]

We can separate the crystalline orientation (Δn_c) and the amorphous one (Δn_a) from an overall molecular orientation (Δn) by formulas (1) and (2).

$$\Delta n = \Delta n_c X + \Delta n_a (1 - X) \qquad (1)$$

$$\Delta n_c = f_c \Delta n_o \qquad (2)$$

where X = volume crystallinity, f_c = crystal orientation factor, and Δn_o = intrinsic birefringence.[15]

Figure 7 shows Δn_c and Δn_a as a function of spinning speed.

Δn_c is very high and increases to 0.25 at 8000–9000 m/min, while Δn_a is very low and reaches maximum 0.05 at 4000–5000 m/min and decreases with increase of spinning speed. The maximum value of $\Delta n = 0.12$ at 7000 m/min is much lower than the value $\Delta n = 0.15$ for conventional FOY, probably because of very low amorphous orientation.

High-speed spun yarn is a fiber characterized by highly oriented crystal and low-oriented amorphous phases.[7,15]

Sheath-Core Structure

This section discusses the characteristic fiber structure developed in high-spinning speed of 8000–10,000 m/min.

Ishizaki et al. reported on the cross-section of PET as-spun yarn at 6000 and 10,000 m/min observed by transmission electron microscopy.[16] The cross-section of 10,000 m/min yarn clearly

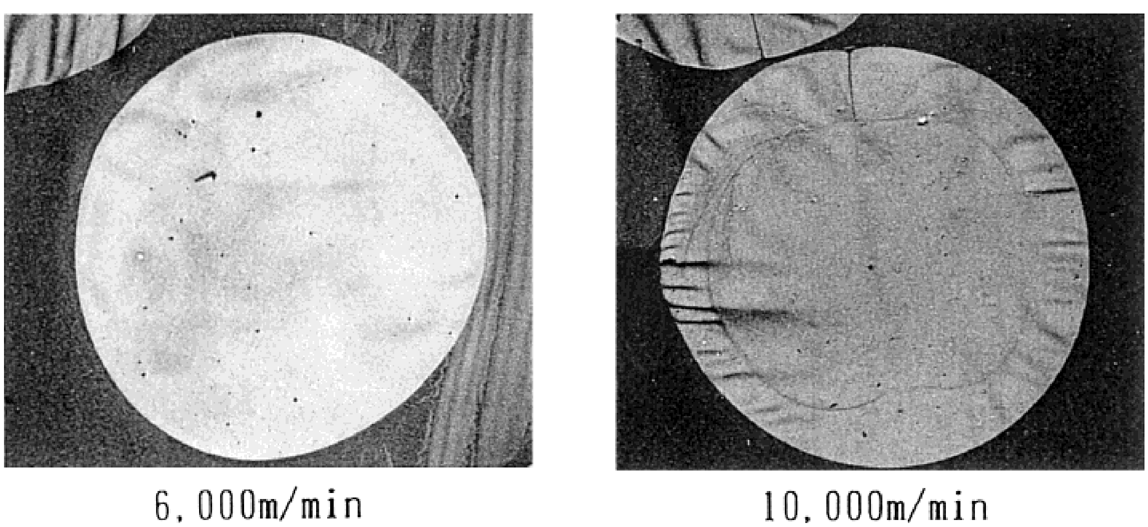

Figure 8 The cross-section of high-speed spun yarn observed by transmission electron microscopy.[16]

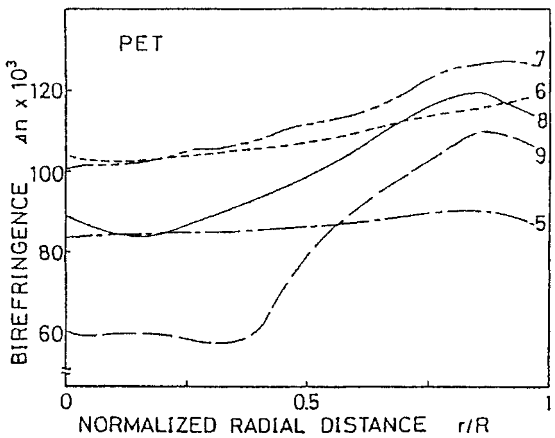

Figure 9 The radial distribution of birefringence in the cross-section of high-speed spun PET yarn.[2,15]

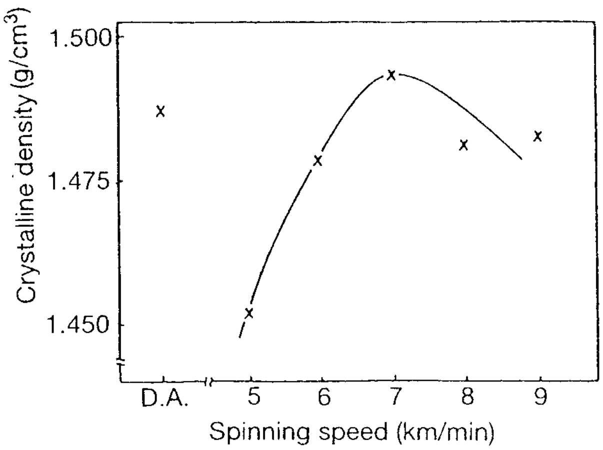

Figure 10 Dependence of crystalline density on spinning speed.[14]

showed a boundary between sheath and core given by osmic acid dyeing.

To analyze the radial variation of the cross-section, the radial distribution of birefringence in a cross-section of yarn was calculated from refractive index parallel and perpendicular to fiber axis.[10]

Figure 9 shows the radial distribution of birefringence in high-speed spun yarn.

At 5000 and 6000 m/min, the difference of birefringence between sheath (r/R = 1) and core (r/R = 0) are relatively small.

At 7000 m/min, birefringence increases throughout the cross-section, and the difference also increases.

At 8000 and 9000 m/min, birefringence considerably drops near the center (core), and slightly decreases near the surface (sheath). The difference reaches about 0.055 at 9000 m/min.

Crystal Structure

Table I shows the Bragg spacing of high-speed spun yarn.

The spacing of (010) and (100) planes decreases with increase of spinning speed, but the spacing of ($\bar{1}$05) plane keeps almost constant.[14]

Figure 10 shows the dependence of crystalline density on spinning speed.

The density increases with spinning speed and reaches maximum at 7000 m/min; that is, the crystal packing is improved by high-speed spinning.

The decreasing of density at 8000 and 9000 m/min may be related to radial variation of the cross-section.

Table II shows the dependence of crystallite size on spinning speed, which also increased with spinning speed. The crystallite size in c-axis analyzed using the ($\bar{1}$03) and ($\bar{1}$05) planes is relatively larger than that of conventional drawn & annealed (D & A) yarn.

The crystal size in radial direction estimated from (010), (100), and (200) planes monotonously increases with increase of spinning speed. The square brackets in Table II also show the number of unit cells stacked in the respective plane, which

Table I The Bragg Spacing of Crystalline Planes[14]

	d_{spacing}				
	(010)	(100)	(200)	($\bar{1}$03)	($\bar{1}$05)
5000 m/min	5.07 Å	3.48 Å	(3.47) Å	3.40 Å	2.11 Å
6000 m/min	5.01	3.44	(3.44)	3.37	2.10
7000 m/min	4.98	3.42	(3.42)	3.37	2.10
8000 m/min	4.99	3.42	(3.42)	3.38	2.10
9000 m/min	4.99	3.42	(3.42)	3.38	2.10
Drown & Annealed	5.04	3.46	(3.45)	3.36	2.10

Table II Crystallite Size of High Speed Spun PET Yarn[14]

	Scherrer's Method			Hosemann's Method			
	(010)	(100)	(200)	(100),(200)	g_{II}	$(\bar{1}03),(\bar{1}05)$	g_{II}
5000 m/min	49.4 Å [9.7]	29.7 Å [7.5]	29.5 Å [8.5]	(29.5) Å	—	66.8 Å [6.2]	1.12%
6000 m/min	59.6 Å [11.9]	49.5 Å [12.6]	46.0 Å [13.4]	47.8 Å [13.9]	4.5%	91.6 Å [8.5]	0.75%
7000 m/min	67.2 Å [13.5]	53.9 Å [13.8]	53.3 Å [15.6]	55.8 Å [16.3]	4.4%	102.9 Å [9.6]	0.71%
8000 m/min	72.1 Å [14.4]	60.9 Å [15.4]	63.9 Å [18.7]	69.0 Å [20.2]	4.5%	115.6 Å [10.8]	0.61%
9000 m/min	81.1 Å [16.3]	69.3 Å [17.6]	65.2 Å [19.1]	72.5 Å [21.2]	4.8%	90.0 Å [8.4]	0.53%
Drawn and annealed	64.1 Å [12.7]	47.8 Å [12.3]	41.0 Å [11.9]	42.1 Å [12.3]	4.4%	60.1 Å [5.6]	0.40%

shows the rate of increase of stacking is much higher in (100) plane than in the (010) plane.

The crystallization of high-speed spinning may start from the particular plane as the aromatic ring is stacked.[14,17]

Figure 11 shows the melting temperature against the reciprocal of crystal size in the c-axis direction.

It is understood from this result that the melting temperature of high-speed spun yarn is very high because of formation of large-sized crystals in the spin line.

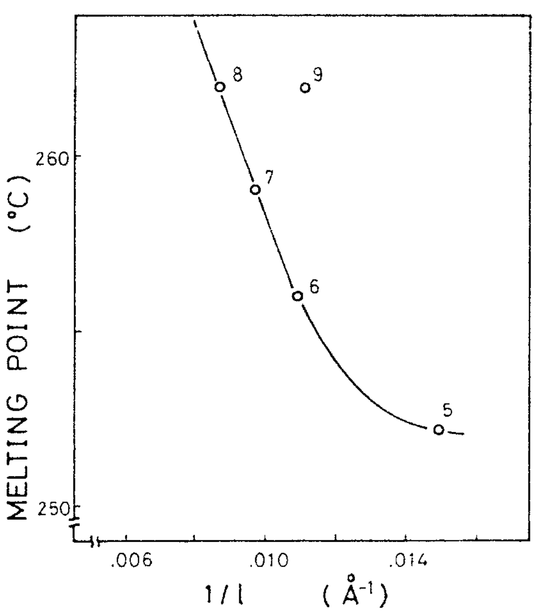

Figure 11 Melting temperature against reciprocal of crystallite size in c-axis.

High Order Structure

The small angle X-ray scattering (SAXS) pattern of high-speed spun PET yarn is changed by drastic changes of high-order structure with increases of spinning speed. Figure 12(a) shows a SAXS pattern of high-speed spun yarn at various speeds and D & A fiber, and Figure 12(b) shows the schematic descriptions. A distinct SAXS pattern appears above 5000 m/min and an x-shaped four-lobe pattern gradually flattens toward the equator with increasing speed. This pattern is very different from the D & A fiber. At 8000–9000 m/min, a diffuse two-spot reflection on the meridian and strong streak on the equator are observed. At 7000 m/min, both patterns are piled on each other.[2,14]

Figure 13(a,b) shows a structure model of 5000 and 9000 m/min yarns simulated consulting the results of WAXS and SAXS measurements.

The model of 5000 m/min shows that the microfibril in the fiber structure is composed of about six crystallite units, which are largely displaced parallel to the fiber axis. Crystallite size is very small. The crystallinity calculated from the model is 29%, which agrees with the one obtained from density.

The fibril of 9000 m/min is composed of about two large crystallite units, whose parallel displacement along the fiber axis is very small.

The crystallinity is 75%, which is much greater than the one from density. We believe that the difference results from neglect of: 1. void scattering on the equator, and 2. large radial variation of the cross-section.[17]

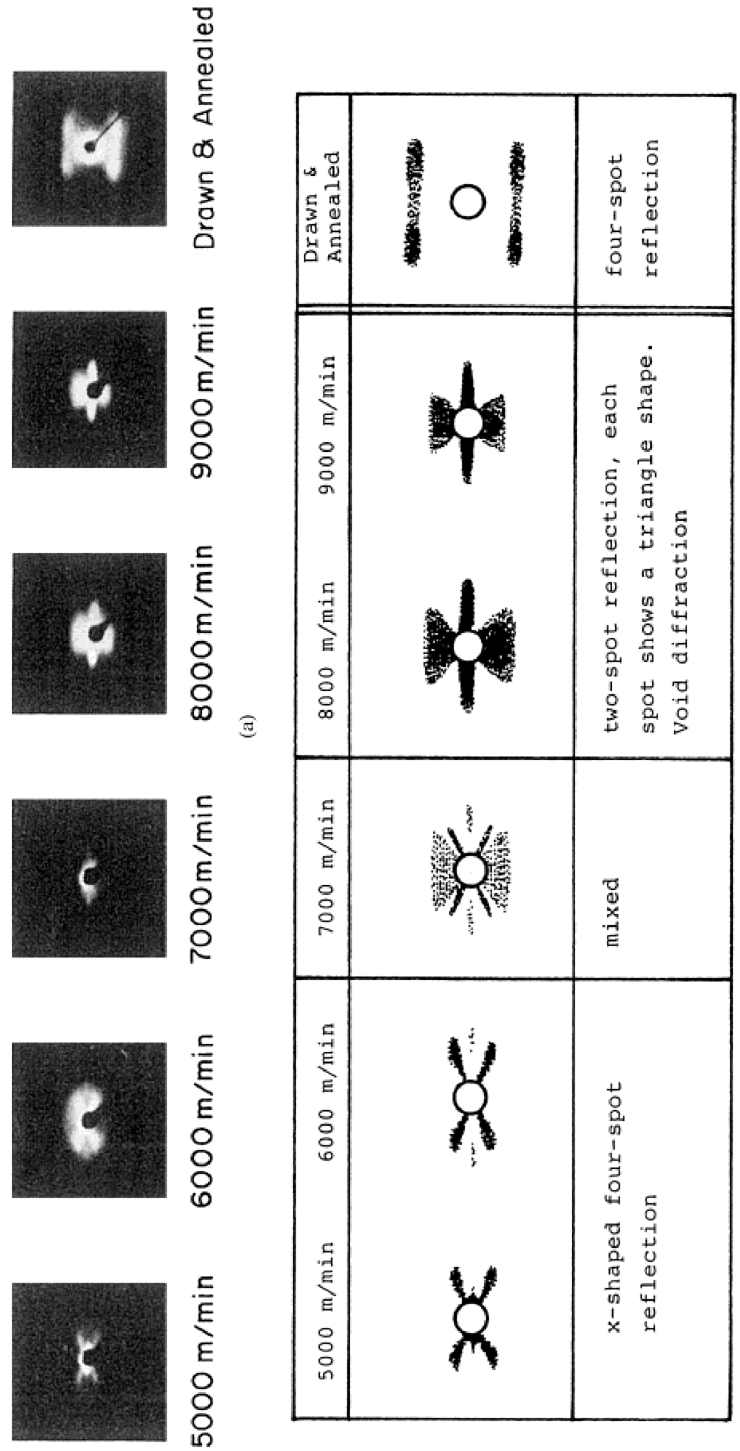

Figure 12 (a) SAXS pattern of high-speed spun and D & A yarn. (b) Schematic illustration of SAXS pattern.[2,14]

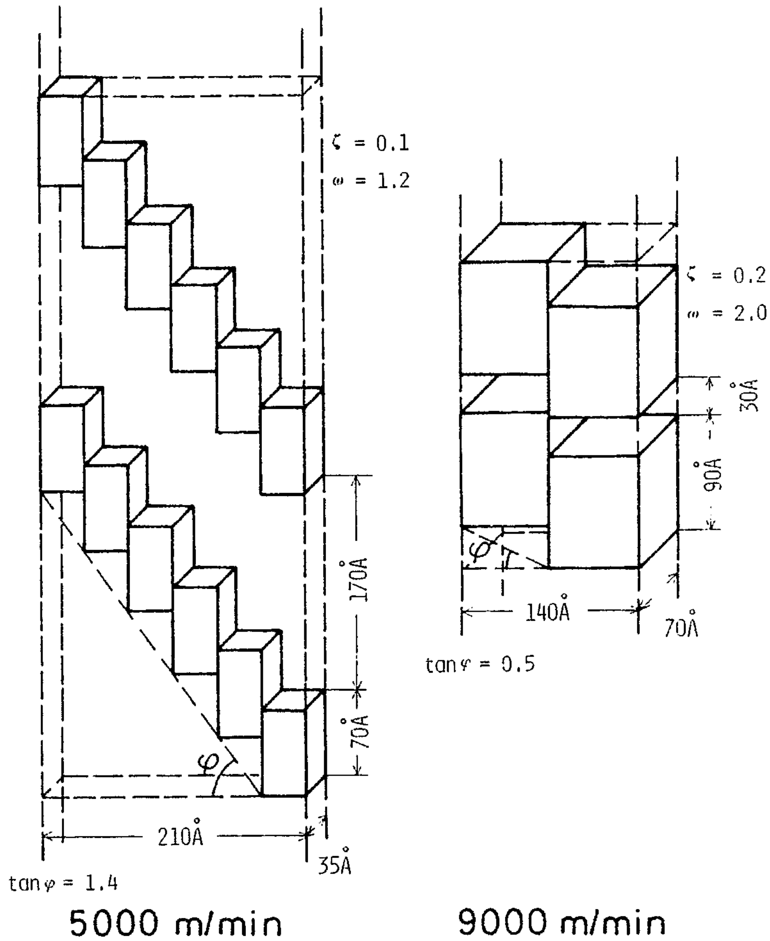

(a) (b)

Figure 13 Structure model of (a) 5000 and (b) 9000 m/min spun PET yarn.[2,14]

Figure 14 shows the intensity on the equator of a SAXS pattern at 5000–10,000 m/min. The distance of inter-microfibril was estimated from this pattern.

The estimated distance is 62 Å at 6000 m/min and 145 Å at 10,000 m/min.

Figure 15 shows the fine structure model on the sheath side of PET fiber at 10,000 m/min.[16,18]

Oriented Mesophase

To discuss further details of the mechanism of orientation-induced crystallization in the spin line, it is best to analyze the dependence of the WAXS pattern on spinning speed more carefully. As can be seen in Figure 4, the WAXS pattern at 4000 m/min shows diffuse reflection on the equator, which suggests that a considerable orientation of molecular chain in the fiber is formed. Sotton et al. designated the structure corresponding to anisotropic diffuse reflection as an "oriented mesophase."[19]

Figure 16 shows the amount of crystalline, oriented meso- and amorphous phases evaluated by WAXS intensity of as-spun yarn.

At 1000–4000 m/min, the amount of oriented mesophase increases and reaches maximum at 4000 m/min.

Above 5000 m/min, the crystalline phase starts to appear and increases until 7000 m/min.

The sum of crystalline and mesophase index may be assumed as the amount of "ordered structure." Such ordered phase increases with increases of spinning speed. Above 5000 m/min, oriented molecules in the mesophase aggregate and initiate the nucleation of crystallization under certain conditions.

In comparison with the D & A yarn, high-speed spun yarn is characterized as a fiber having a small amount of oriented amorphous phase.

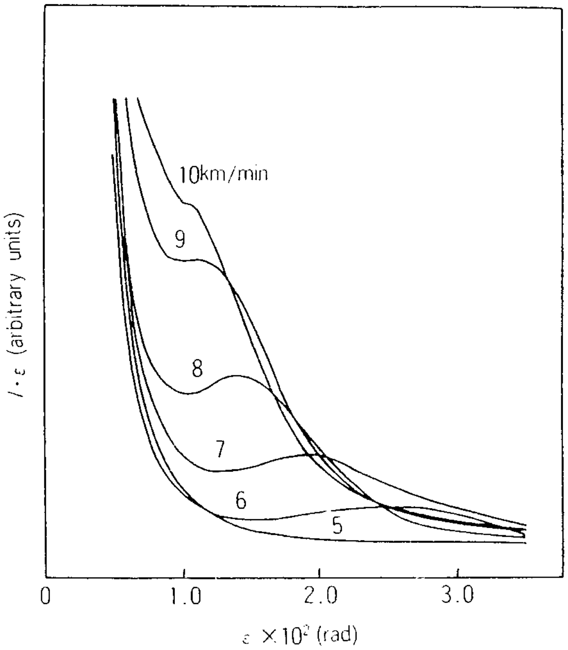

Figure 14 Equatorial intensity from SAXS pattern at various speeds.[16,18]

DYNAMICS OF HIGH-SPEED SPINNING

The formation of fiber structure in high-speed spinning occurs through neck-like deformation and orientation-induced crystallization. And it is confirmed by observation of the change of structure or property on the spin line. Many excellent theoretical and experimental studies have been reported, such as dynamics and simulation of spinning,[20–22] X-ray observation,[23,24] measurement and analysis of physical properties,[23,25] etc.

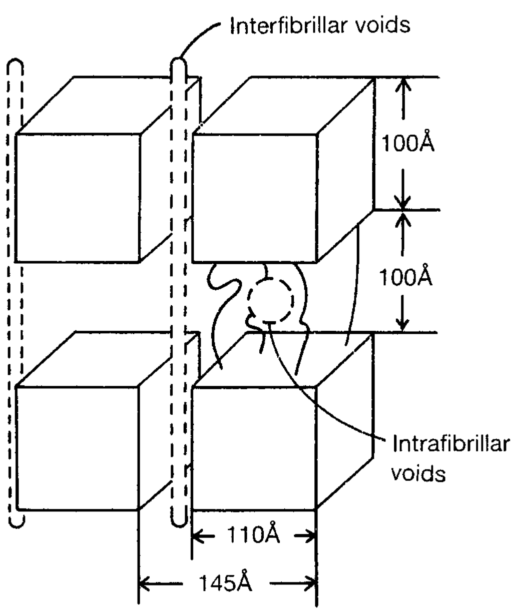

Figure 15 Fine structure model of 10,000 m/min PET fiber.[16,18]

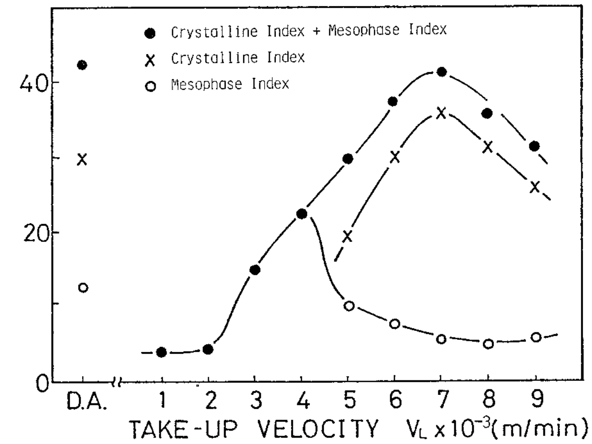

Figure 16 Phase diagram of crystalline, oriented meso- and amorphous for as-spun PET yarn versus spinning speed.[10]

Neck-Like Deformation

Measurement of Neck-Like Deformation

The existence of a neck-like deformation in the spin line was reported by Perez and Lecluse,[25] Matsui,[25] and Shimizu.[27] Recently, Kikutani[28,29] tried the direct observation of necking in the spin line as shown in Figure 17. The diameter profile of necking yarn observed in the spin line is sig-

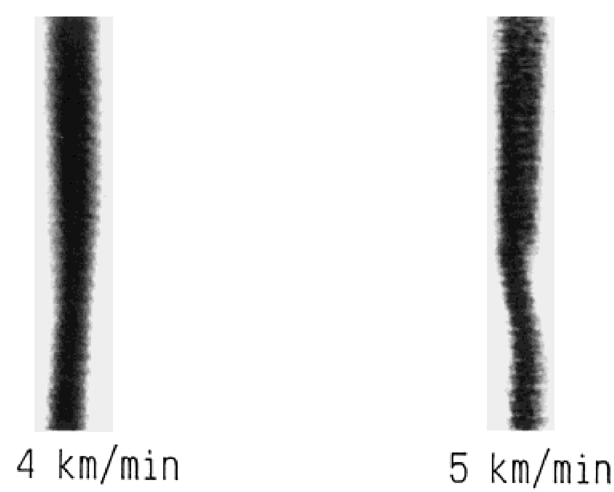

Figure 17 Neck-like deformation of poly(butylene terephthalate) yarn observed in the spin line.[28,29] Magnification in the horizontal direction is 16 times larger than that in the vertical direction.

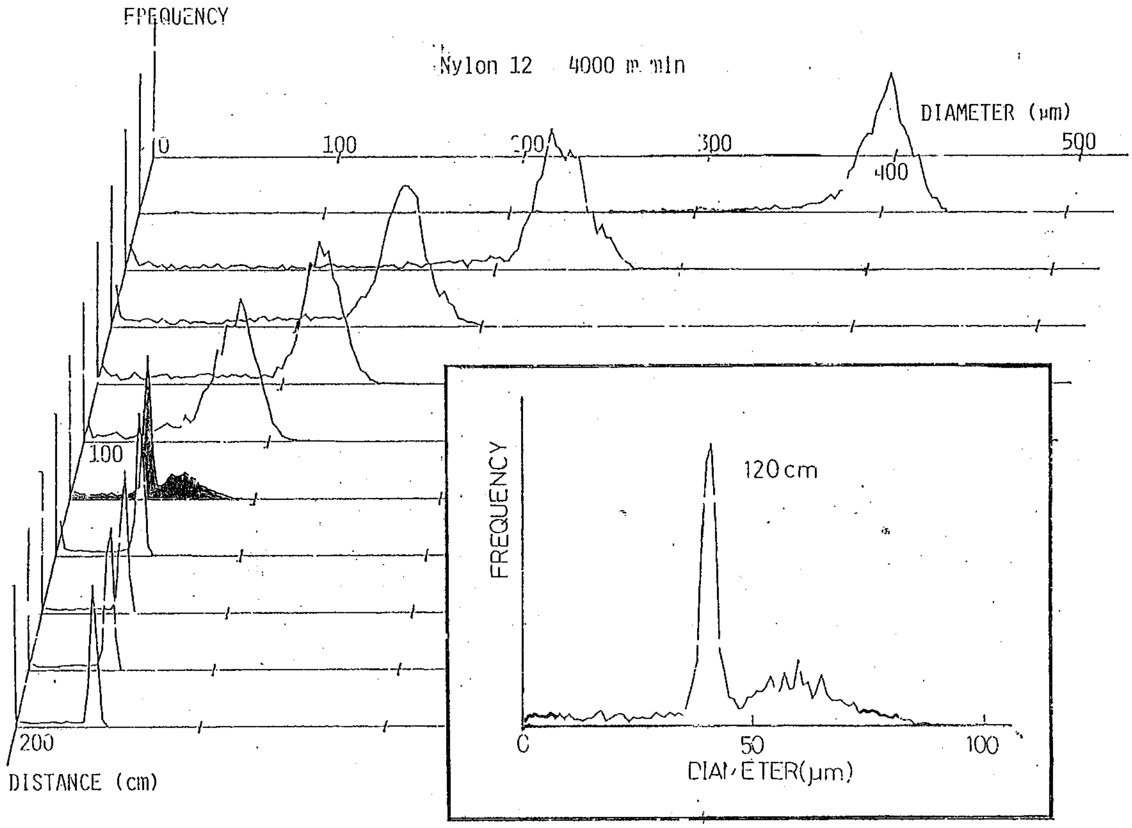

Figure 18 The diameter distribution of nylon-12 spinning yarn measured along the spin line.[17]

nificantly different from the necking in the drawing process or that cut away from running yarn.[26]

To measure the diameter of a spin line and specify a necking position, the diameter monitoring system is composed as follows: running yarn → diameter monitor → DC amp. → D/A converter → computer → diameter distribution and necking position.

Figure 18 shows the diameter distribution of nylon-12 yarn monitored by this system. x-Axis, diameter (μm); y-axis, distance from spinneret; z-axis, frequency diagram of diameter.

From the diameter distribution of the running yarn along the spin line the following characteristics can be noted.

1. The mean diameter decreases monotonously along the spin line up to a certain point (at 120 cm of the y-axis). However, the variation of diameter is very large, that is, the yarn does not yet solidify and is unstable.
   We call such a yarn a liquid yarn, which is a coarse yarn and very uneven.
2. There is the solidification point at 120 cm. Below this point, the distribution becomes sharp; that is, the thinning of a yarn almost stops and reaches the diameter of as-spun yarn.
3. At the solidification point, we frequently recognize a distribution having two peaks, which means that two kinds of coarse and fine yarn are observed by turns. We designate such statistical phenomena as a neck-like deformation (necking).

Necking of PET Spinning

Figure 19(a,b) shows the degree and the position of neck-like deformation (neck or necking) of PET yarn at various spinning conditions.

Necking occurs in a very narrow region (necking zone). We designated the following parameters at the entrance and exit of the necking zone.

	Entrance	Exit
Cross-section area	A_1	A_2
Velocity	V_1	V_2
Density	ρ_1	ρ_2

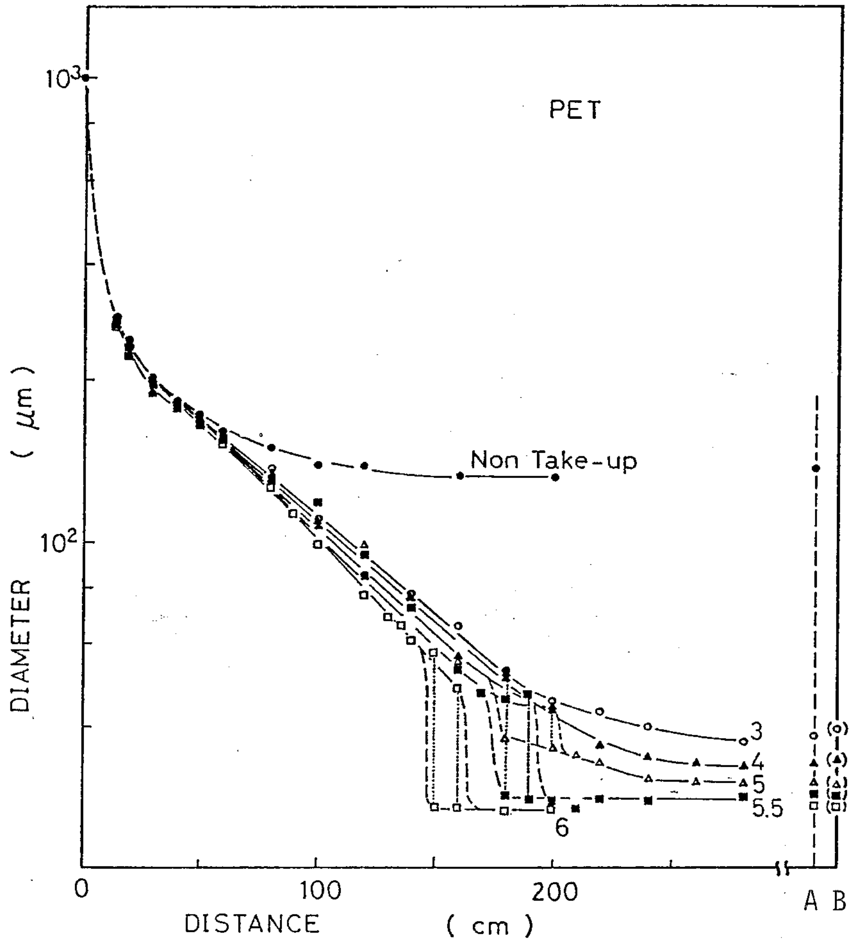

(a)

Figure 19 (a) Diameter profiles of PET yarn in high-speed spin line of various spinning velocities (km/min). (b) diameter profiles of PET 6000 m/min yarn at various throughput rates.[10]

from the material balance equation, $\rho_1 A_1 V_1 = \rho_2 A_2 V_2$.

$$\text{And if } \rho_1 = \rho_1, \quad v_2/v_1 = A_1/A_2 \qquad (3)$$

Equation (3) is called the necking draw ratio, which increases with spinning speed and the neck point moves toward the upstream with spinning speed.

Table III shows the temperature of solidification point of PET and other polymers. The necking temperature increases with spinning speed. But for every spinning condition of every polymer, the temperature of solidification point is significantly lower than the melting point of each polymer.

In other words, necking starts in the condition of super cooling.

Figure 19(b) shows the dependence of necking on various throughput rates at 6000 m/min of high-speed spinning. The necking point moves upstream and the necking draw ratio increases with a decrease of throughput rate.[20]

Despite high speed, many kinds of polymers can be spun because of such high spinability, which will be discussed later.

Figure 20 shows the profile of output voltage of an infrared radiation gauge and the diameter along the spin line.[25,30]

This figure shows crystallization starts just before or after necking.

Mechanism of Neck-Like Deformation

Fujimoto et al. investigated the mechanism of necking by physical values obtained from diameter profile of a running yarn as shown in Figure 21(a).[5,24]

Figure 21(b) shows the velocity gradient of deformation dV/dX along a spin line at 4000–10,000

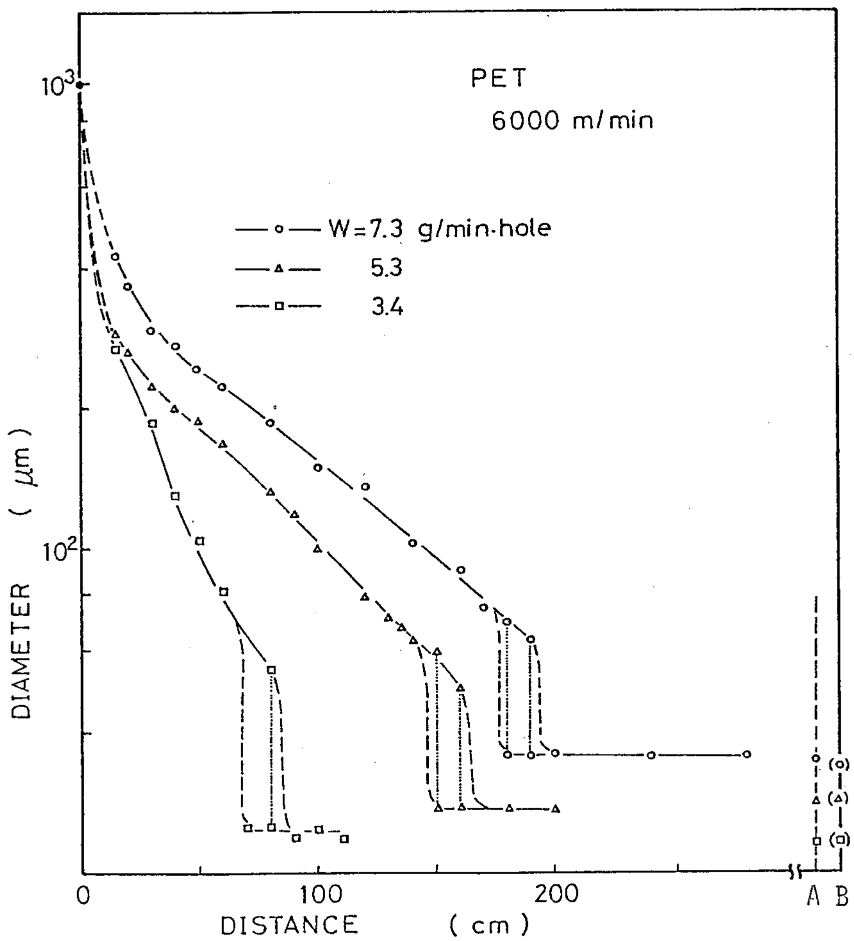

(b)

Figure 19 (*Continued from the previous page*)

m/min spinning. dV/dX reaches a maximum at necking point, which becomes higher with an increase of spinning speed[5]: spinning speed, 4000 m/min; velocity gradient, 100 s^{-1}; spinning speed, 10,000 m/min; velocity gradient, 1500 s^{-1}.

Kikutani[28,29] reported new data that, as the deformation proceeded to the end point of the point, the velocity gradient rapidly increased to

Table III Calculated Temperature at Starting Point of Necking[10,17]

	Take-up Velocity (m/min)					
Polymer	2000	3000	4000	5000	5500	6000
PP		67°C	114°C	114°C		
Nylon 12		90°C	102°C	135°C		
PET				102°C	123°C	148°C

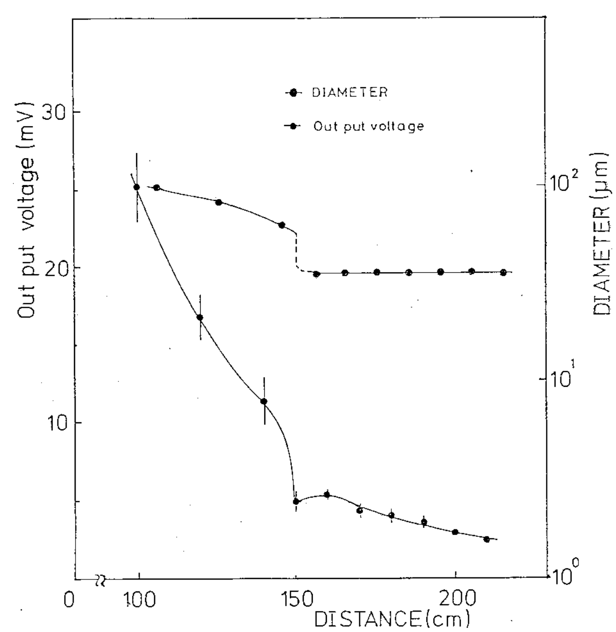

Figure 20 Heat generation caused by crystallization and necking position.[25,30]

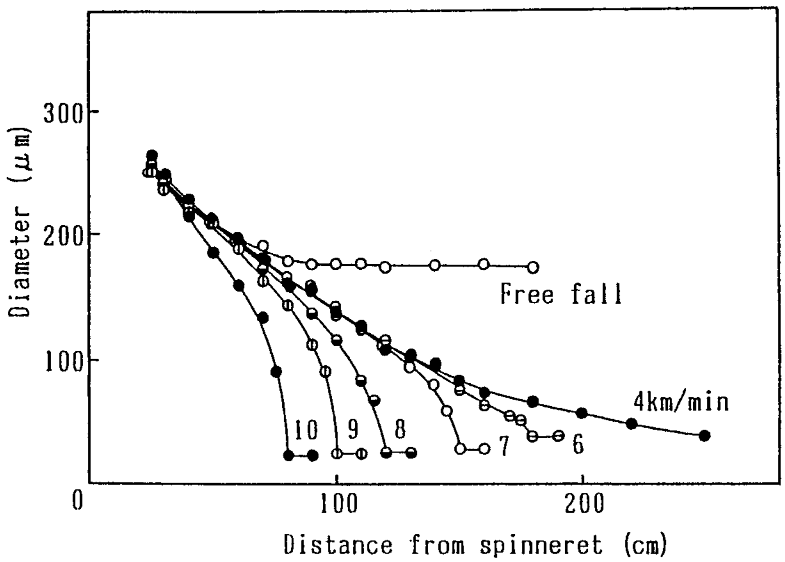

(a)

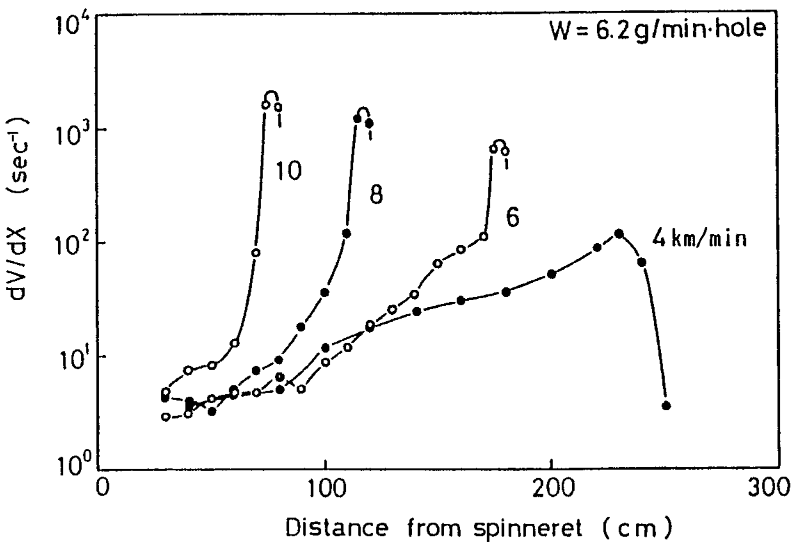

(b)

Figure 21 (a) Diameter profile along a spin line at various speeds. (b) Velocity gradient *dV/dX* along a spin line obtained from (a). (c) Spinning stress (σ) along a spin line. F_L is measured. (d) Elongational viscosity (η) calculated from the data of (b) and (c).[31]

ca. 10,000–30,000 s^{-1} at a spinning speed of 4000–5000 m/min, respectively.

The spin line tension is given by the equation,[18,22]

$$F = F_L + \int_x^L \rho A g \, dx - W(V_L - V) - \int_x^L C_f(\rho_a/2)V^2 \pi D \, dx \quad (4)$$

$$C_f = 0.37 \text{ Re}^{-0.61} \quad (5)$$

where F, F_L = spinning tension at x below the spinneret and at take-up point L; C_f = air drag coefficient; Re = Reynolds number; 2nd term = gravity force; g = acceleration of gravity; 3rd term = inertia force; W = throughput rate; 4th term = air drag, ρ_a = air density; D = diameter.

From eq. (4), it is understood that[20,24]: (a) spin line tension F increases along a sigmoid path until solidification point, and beyond this point F linearly increases toward take-up tension F_L; (b)

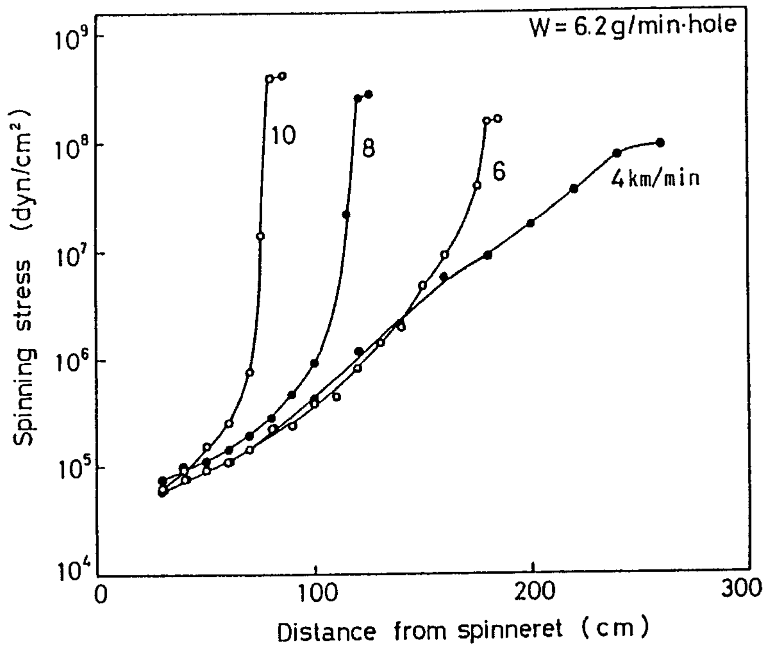

(c)

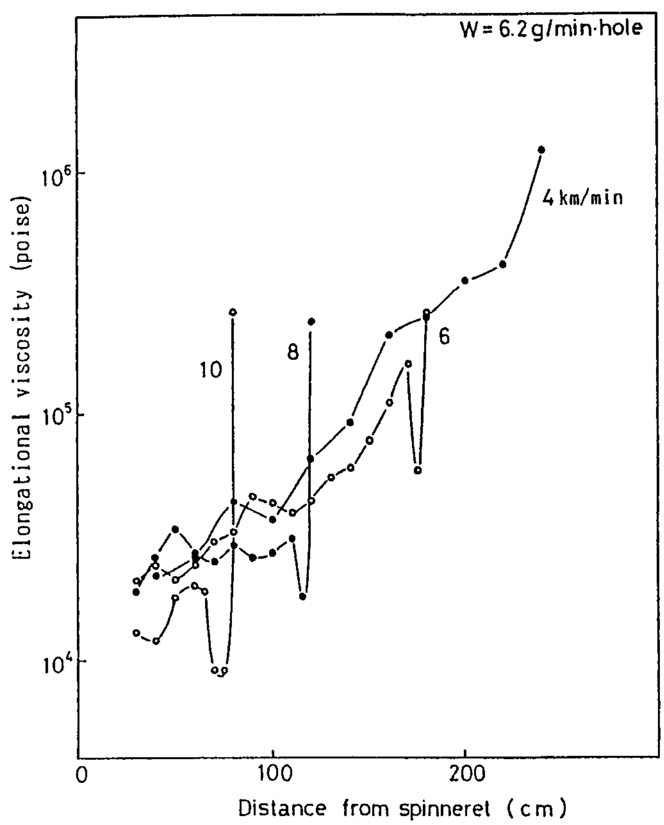

(d)

Figure 21 (*Continued from the previous page*)

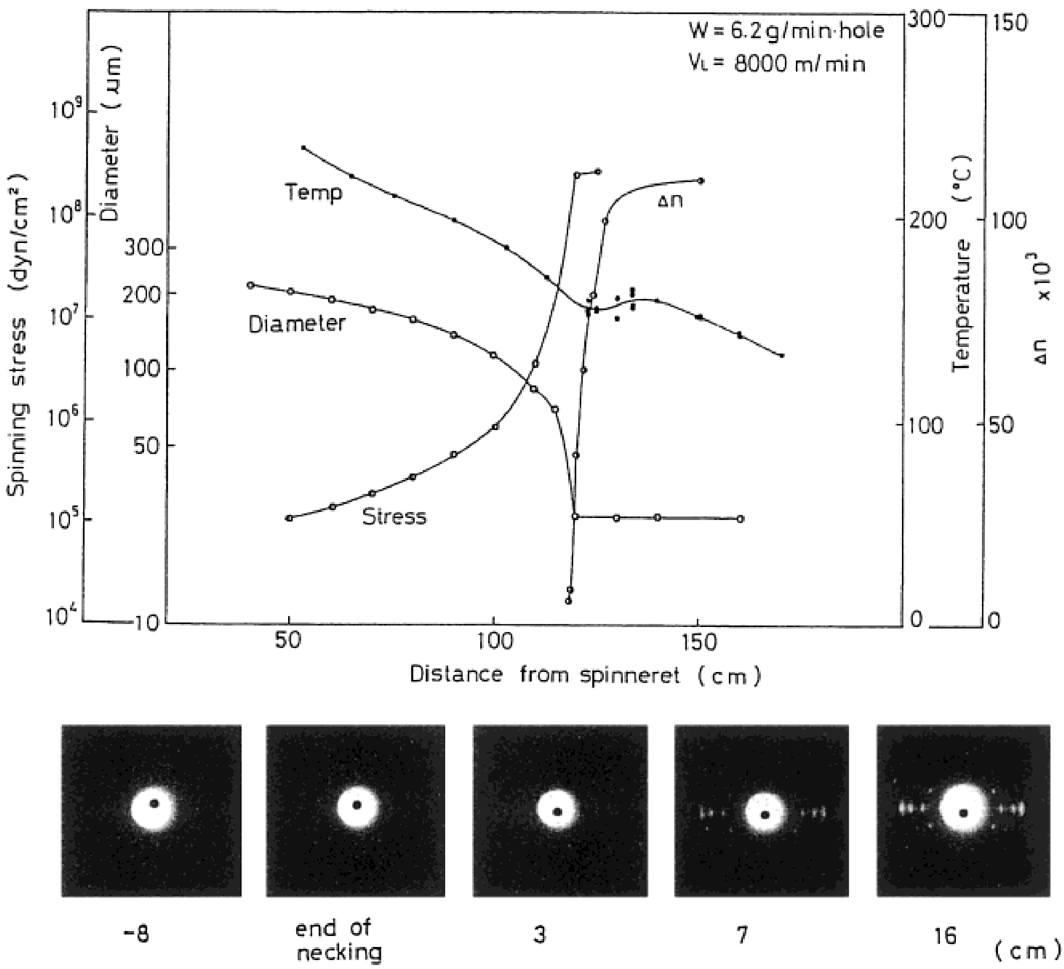

Figure 22 Diameter, temperature, spinning stress, and birefringence along a spin line of 8000 m/min and related WAXS pattern.[32,33]

So the increase of inertia force seems to contribute to a yarn formation in liquid state.

Figure 21(c) shows the spinning stress (σ) calculated by eq. (4).

The stress increases in the order from 10^6 to 10^8 dyne/cm^2.

The apparent elongational viscosity (η) can be evaluated from the rheology equation as follows:

$$\sigma = \eta(dV/dx) \tag{6}$$

Figure 21(d) shows the behavior of elongational viscosity along a spin line at various spinning speeds.

The viscosity monotonously increases along a spin line in the case of 4000 m/min. But at 6000 m/min, the monotonous increase stops at a certain point ($x \fallingdotseq 170$ cm), and the viscosity locally drops, and after dropping it steeply climbs.

Such a behavior was observed in 8000 and 10,000 m/min, and the start of neck-like deformation seems to correspond with a localized viscosity drop.[18]

We speculated that the formation of oriented mesophase might bring the above localized viscosity drop.

Crystallization in Spin Line

The crystallization of high-speed spinning is greatly accelerated by molecular orientation forced by spinning tension. To analyze the crystallization, the Avrami equation is modified to apply to the nonisothermal crystallization as follows.[20,21]

$$X = 1 - \exp\left\{-\left(\int_o^t K(T, \Delta n)\, dt'\right)^n\right\} \tag{7}$$

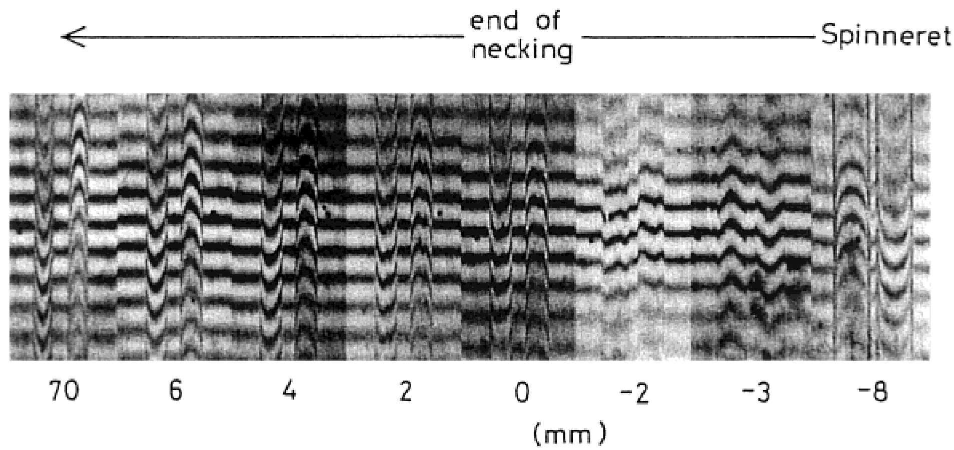

Figure 23 Fringe pattern observed by interference microscope near necking of 6000 m/min yarn captured from spin line.[16,32]

where K = rate constant of crystallization given by a function of temperature T and Δn. K shows a maximum between glass transition T_g and a melting point T_m.

K increases with an increase of orientation Δn.

We generally recognize that the molecular orientation or crystallization in high-speed spinning is occurring near the necking or through the necking. However, it is very difficult to get precise information from the dynamic process.

To solve this problem, we need several investigations as follows.

1. Precise measurement of physical properties related to structural changes and simultaneous measurement of some mechanical characteristics at the same position.[17,31] 2. Information from other polymers having a very different nature from PET, such as PP, NY, PS, etc.[2,34–37]

The increase of temperature caused by crystallization after necking was described previously. Figure 22 shows, in the case of 8000 m/min, the changing of the WAXS pattern in the spin line with increases of birefringence, diameter thinning, and its necking position. The result given by Fujimoto is very interesting as discussed below.[3,12]

At 4000 m/min, the increase of Δn and the diameter thinning cease simultaneously. However, at 8000 m/min, Δn is very small at the end point of necking ($\Delta n = 0.03$ at $x = 0$), and increases abruptly after necking and goes up to $\Delta n = 0.11$.

The WAXS pattern shows only an amorphous halo at $x = -8$ cm, and a very weak reflection spot just after neck at $x = 0$.

Distinct reflection spots are observed from $x = 7$ cm of downstream and a complete PET WAXS pattern is observed at $x = 16$ of downstream.

Matsui[22] and Hirahata et al.[24] tried to directly observe orientation-induced crystallization during high-speed spinning of 6000 and 4000 m/min by WAXS.

According to Matsui,[22] the increase of orientation ($\Delta n = 0.02$–3) starts under process of necking, and reaches a maximum value after necking. The Bragg reflection from crystallites is clearly observed from $x =$ ca. 10 cm.

Hirahata et al.[24] reported that the width of the necking zone is ca. 75 mm, in which a yarn diameter changes from 60 to 27 μm. From the starting position of its necking, the oriented crystal reflection is observed, but it is very weak. A clear crystal reflection is observed from $x = 20$ cm of downstream. They say, "Orientation induced crystallization starts before the end of necking deformation, which is followed by further crystal growth. It also can be supposed that necking deformation is caused by the appearance of the locally oriented molecular chain in a fiber."

Another important factor of crystallization is the effect of cooling.

As already shown in Figure 9, the PET yarn spun at 8000 and 9000 m/min has a radial variation of structure in cross-section due to rapid cooling. And the figure also shows that the 6000 m/min spun yarn has a homogeneous cross-section.[10,20]

Figure 23 is a yarn captured from the spin line of 6000 m/min and observed under an interference microscope. $x = 0$ is the end point of necking, $x = -8$ mm is upstream of the neck, and $x = 70$ mm is downstream.

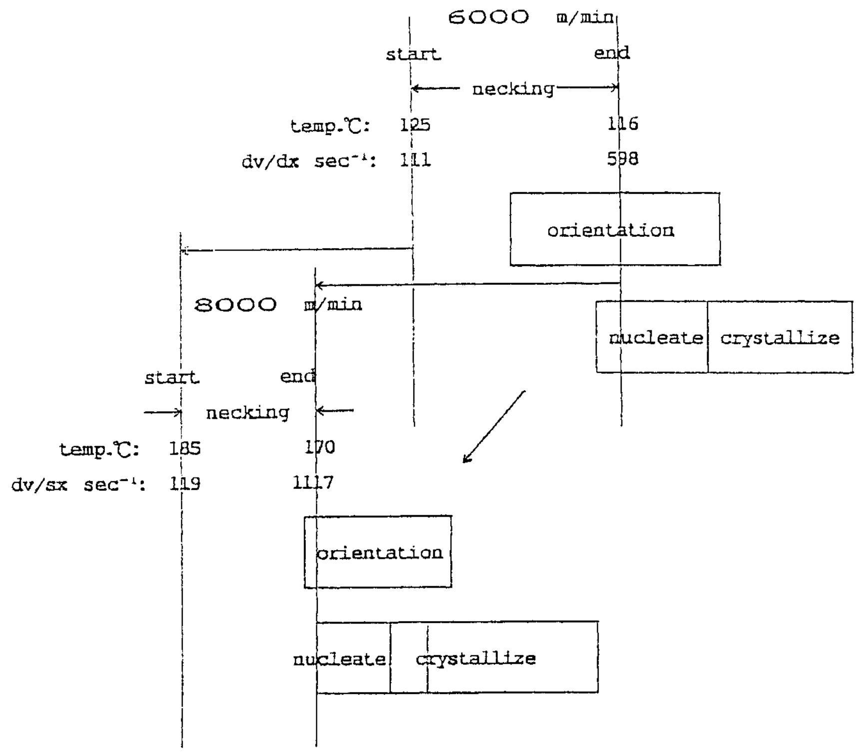

Figure 24 Comparison of 8000 m/min with 6000 m/min in terms of relations between necking and crystallization.[17]

The 6000 m/min spun yarn at $x = -8$ mm shows a parabolic fringe pattern, which means it has a homogeneous cross-section.

Crystallization starts from the yarn surface just before the end point $x = 0$ of necking, and then the center of the parabolic fringe is caved in. This tendency is enlarged with the progress of crystallization. At $x = 2$ mm, the center of parabola turns to the opposite direction, and at $x = 70$ mm, a complete parabola is formed again.

The sheath-core structure is also made by extremely rapid cooling.[2]

Consideration of Neck-Like Deformation

The cause of necking and stability of spinning can be summarized as follows.

Cause of Necking

The direct observation of necking yarn on a spin line is very difficult.

Therefore, many problems are not yet solved. One question is how a liquid yarn is super-drawn.

1. Diameter gradient is very small, $dD/dx \leqq$ ca. 0.01.

This means deformation is done under simple uniaxial elongation.[28,29] But velocity gradient is very large, and the time of necking is extremely short, $dV/dx \geqq 10^3\ s^{-1}$. 2. Spinning tension at necking deformation is dominated by inertia force, where apparent viscosity is dropping locally.

Another question is why the change of such behavior in liquid occurred. This is unknown, and requires an answer.

We have already described it as follows. 1. Owing to formation of oriented mesophase at $\Delta n \geqq 0.03$ of 3000 m/min, some molecules in the mesophase aggregate to make a nucleus. 2. When the amount of mesophase reaches a certain value, crystallization occurs under high spinning stress and a large temperature gradient.

Comparing 8000 m/min with 6000 m/min, such relations are summarized in Figure 24.

In the figure, the starting and ending point of necking goes up, necking zone becomes narrow, but nucleation and crystallization go to downstream. The stages of orientation, nucleation, and crystallization are overlapping one another.

Stability of Spinning

The stability of spinning is a very important factor concerning industrial technology.

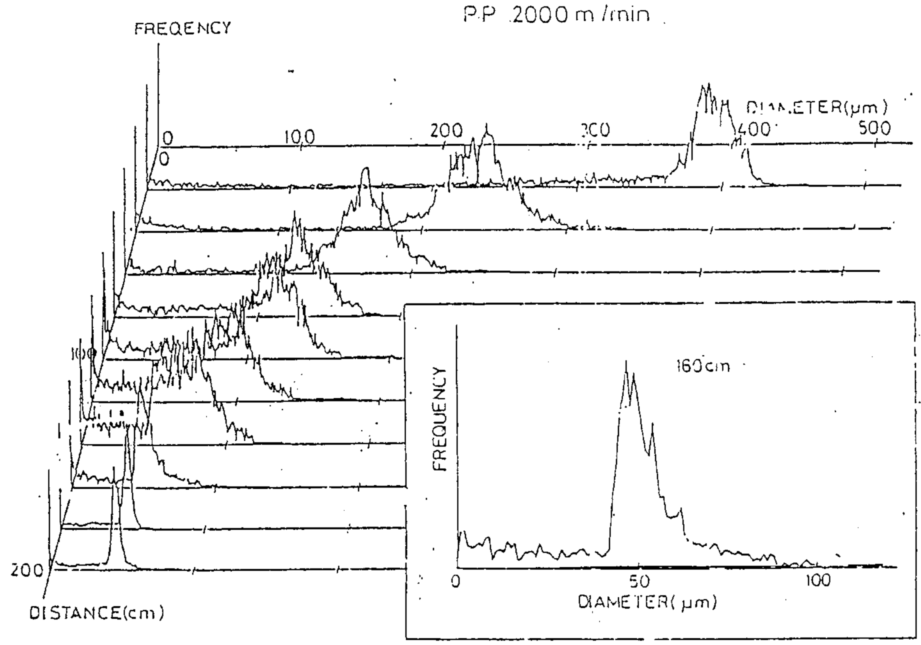

(a)

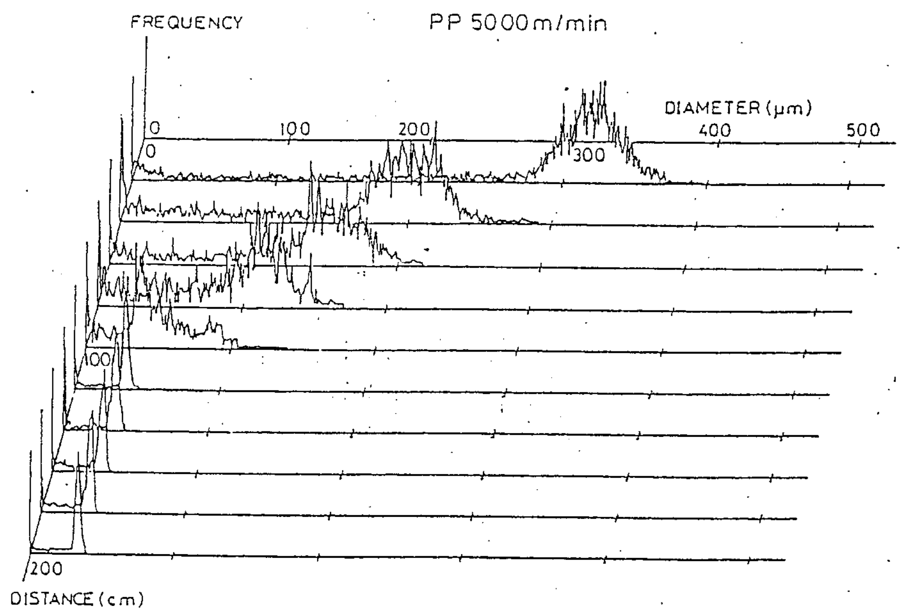

(b)

Figure 25 Diameter distribution of PP spinning yarn. (a) 2000 m/min, (b) 5000 m/min.

Figure 25(a,b) shows the diameter distribution along the spin lines of PP spinning yarn at 2000 and 5000 m/min.[25]

From the figure, we see that each spinning yarn has both regions of very even yarn in solid state and very uneven yarn in liquid state, which is divided at a position of neck-like deformation. In the case of PP spinning yarn of 2000 m/min, the necking position is in 160–180 cm of a spin line. In the case of 5000 m/min, the necking position moves up and is observed in 100–120 cm of the spin line. The regularity of yarn diameter seems to be controlled by passing through the necking position.

We conclude that the stability of spinning is as follows.

According to a coarse or a fine part of a liquid yarn, the necking position goes down or goes up to keep a certain tension balance; therefore, the tension balance between liquid and solid yarn may be governed by the moving of the position in necklike deformation. We think that molecular orientation and induced crystallization are very important factors to get a high regularity yarn. This is a characteristic of high-speed spinning.

We are grateful to Dr. M. Matsui and Dr. K. Fujimoto for much helpful advice and collaboration. We thank Prof. K. Toriumi, Mr. K. Tamai, Prof. N. Okui, Mr. A. Kaneko, Dr. S. Terui, and Dr. Y. Kawahara, for performing experiments used in this research.

REFERENCES

1. Carothers, W. H. Collected Papers on High Polymeric Substances; Interscience: New York, 1940.
2. Shimizu, J.; Okui, N.; Kikutani, T. High-Speed Fiber Spinning; John Wiley & Sons: New York, 1985; p 429.
3. du Pont. Pat. 1960-3104.
4. Ziabicki, A. Kolloid-Z 1961, 175, 14.
5. Murase, Y.; Nagai, A. Advanced Fiber Spinning Technology; Woodhead Publishing: Cambridge, 1994; p 25.
6. Shimizu, J. Sen-i Gakkaishi 1978, 34, T-93.
7. Shimizu, J.; Toriumi, K.; Tamai, K. Sen-i Gakkaishi 1977, 33, T-208.
8. Shimizu, J.; Okui, N.; Kikutani, T.; Toriumi, K. Sen-i Gakkaishi 1978, 34, T-93.
9. Shimizu, J.; Okui, N.; Kaneko, A.; Toriumi, K. Sen-i Gakkaishi 1978, 34, T-64.
10. Kikutani, T. Ph.D. Thesis, Tokyo Institute of Technology, 1982.
11. Shimizu, J.; Okui, N.; Terui, S.; Annual Meeting of the Society of Fiber Science and Technology, Japan 1979; p 5.
12. Sen-i Binran (Handbook on Fibers) 2nd ed.; Maruzen: Tokyo, 1994; p 848.
13. Daubeny, R. de D.; Bunn, C. W.; Brown, C. J. Proc Roy Soc (London) 1954, A226, 531.
14. Shimizu, J.; Kikutani, T.; Takaku, A.; Okui, N. Sen-i Gakkaishi 1984, 40, T-63.
15. Shimizu, J.; Okui, N.; Kikutani, T. Sen-i Gakkaishi 1981, 37, T-135.
16. Ishizaki, S.; Iohara, K.; Fujimoto, K. Sen-i Gakkaishi 1989, 45, P-234.
17. Shimizu, J. Sen-i Kikai Gakkaishi 1985, 38, 243.
18. Fujimoto, K. Ph.D. Thesis, Tokyo Institute of Technology, 1989.
19. Sotton, M.; Arniaud, A. M.; Rabourdin, C. J Appl Polym Sci 1978, 22, 954.
20. Shimizu, J.; Okui, N.; Kikutani, T. High-Speed Fiber Spinning; John Wiley & Sons: New York, 1985; p 173.
21. Katayama, K. Advanced Fiber Spinning Technology; Woodhead Publishing: Cambridge, 1994; p 25.
22. Matsui, M. Ph.D. Thesis, Kyoto University, 1996.
23. Matsui, M. Sen-i Gakkaishi 1982, 38, 508.
24. Hirahata, H.; Yabuki, K.; Seifert, S.; Zachmann, H. G. "BENIBANA" International Conference on High Speed Spinning; 1994; p 10.
25. Kawahara, Y. Master's Thesis, Tokyo Institute of Technology, 1985.
26. Perez, G.; Lecluse, C. Proceedings of the 18th International Man-Made Fiber Conference, Dornbirn, 1979.
27. Shimizu, J. Sen-i Gakkaishi 1982, 38, 499.
28. Kikutani, T. "BENIBANA" International Conference on High Speed Spinning; 1994; p 7.
29. Kikutani, T.; Kawahara, Y.; Ogawa, N.; Okui, N. Sen-i Gakkaishi 1994, 50, 561.
30. Kikutani, T.; Kawahara, Y.; Matsui, T.; Takaku, A.; Shimizu, J. Seikei-Kakou 1989, 1, 333.
31. Fujimoto, K.; Iohara, K.; Ohwaki, S.; Murase, Y. Sen-i Gakkaishi 1988, 44, T-53.
32. Matsui, M. "BENIBANA" International Conference on High Speed Spinning; 1994; p 14.
33. Fujimoto, K.; Iohara, K.; Ohwaki, S.; Murase, Y. Sen-i Gakkaishi 1988, 44, T-177.
34. Shimizu, J.; Okui, N.; Kikutani, T.; Ono, A.; Takaku, A. Sen-i Gakkaishi 1981, 37, T-143.
35. Imai, Y. Ph.D. Thesis, Tokyo Institute of Technology, 1981.
36. Shimizu, J.; Okui, N.; Imai, Y.; Nishide, S.; Takaku, A. J Polym Sci Phs Ed 1983, 22, 275.
37. Fujimoto, K.; Iohara, K.; Ohwaki, S.; Murase, Y. Sen-i Gakkaishi 1988, 44, T-395.